Applied Physics Letters

MOCVD growth of $MgGa_2O_4$ thin films for high-performance solar-blind UV photodetectors

Cite as: Appl. Phys. Lett. **120**, 011101 (2022); https://doi.org/10.1063/5.0077904
Submitted: 08 November 2021 • Accepted: 15 December 2021 • Published Online: 03 January 2022

Qichao Hou, Kewei Liu, Dongyang Han, et al.

COLLECTIONS

Paper published as part of the special topic on Wide- and Ultrawide-Bandgap Electronic Semiconductor Devices

ARTICLES YOU MAY BE INTERESTED IN

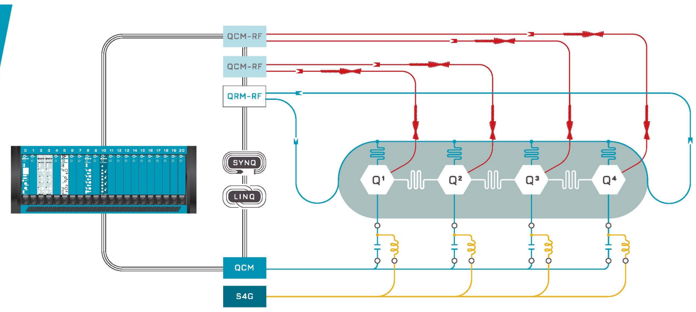

AIP Publishing

MOCVD growth of $MgGa_2O_4$ thin films for high-performance solar-blind UV photodetectors

Cite as: Appl. Phys. Lett. **120**, 011101 (2022); doi: 10.1063/5.0077904
Submitted: 8 November 2021 · Accepted: 15 December 2021 · Published Online: 3 January 2022

View Online Export Citation CrossMark

Qichao Hou,[1,2] Kewei Liu,[1,2,a)] Dongyang Han,[1,2] Yongxue Zhu,[1,2] Xing Chen,[1,2] Binghui Li,[1,2] Lei Liu,[1,2] and Dezhen Shen[1,2,a)]

AFFILIATIONS

[1]State Key Laboratory of Luminescence and Applications, Changchun Institute of Optics, Fine Mechanics and Physics, Chinese Academy of Sciences, Changchun 130033, People's Republic of China

[2]Center of Materials Science and Optoelectronics Engineering, University of Chinese Academy of Sciences, Beijing 100049, People's Republic of China

Note: This paper is part of the APL Special Collection on Wide- and Ultrawide-Bandgap Electronic Semiconductor Devices.
[a)]**Authors to whom correspondence should be addressed:** liukw@ciomp.ac.cn and shendz@ciomp.ac.cn

ABSTRACT

Epitaxial $MgGa_2O_4$ thin films with a bandgap of 5.18 eV were grown on the *c*-plane sapphire substrate by using metal organic chemical vapor deposition. The structure, optical, electronic, and optoelectronic properties of $MgGa_2O_4$ thin films have been investigated before and after high-temperature annealing in an oxygen or nitrogen atmosphere. In particular, the O_2-annealed $MgGa_2O_4$ thin film reveals a high crystalline quality and a low concentration of oxygen vacancies. Moreover, a quick response speed ($t_r = 20$ ns, $t_d = 400$ ns), a low dark current (~17 pA at 10 V), and a high UV/Visible rejection ratio (>10^5) can be demonstrated in the O_2-annealed $MgGa_2O_4$ photodetector, indicating the excellent solar-blind ultraviolet (SBUV) photodetection characteristics. The effect of annealing atmosphere on the photoelectric properties of the film and its physical mechanism were studied. This research provides an effective way to realize high-performance SBUV photodetectors and opens up the application of $MgGa_2O_4$ spinel in the field of semiconductor optoelectronic and microelectronic devices.

Solar-blind ultraviolet (SBUV) photodetectors have attracted much attention due to their inherent advantages of low background noise, high sensitivity, and strong anti-interference ability, which have broad potential applications in both military and civilian fields.[1–3] Until now, various wideband gap (WBG) semiconductors (such as GaAlN,[4–6] ZnMgO,[7,8] and Ga_2O_3[9–11]) have been used to demonstrate the SBUV photodetectors, and some of them have yielded amazing performance. However, the fabrication of high-quality GaAlN[5,12] and ZnMgO[13,14] ternary alloy films usually require harsh conditions, which brings a huge challenge for the development of high-performance SBUV detectors. Meanwhile, multiple deep level defect states within the bandgap are easily formed in Ga_2O_3 and, thus, slow response speed and small UV/Visible rejection ratio have become common problems of Ga_2O_3 SBUV photodetectors.[7] Fortunately, the exploration of materials for preparing high-performance solar-blind photodetectors has never ceased. In recent years, ternary complex oxide WBG semiconductors, such as $ZnGa_2O_4$,[15,16] Zn_2GeO_4,[17] and $In_2Ge_2O_7$,[18] have been intensively studied for SBUV detection because of their ideal bandgap, tunable properties via adjusting the components, high chemical and physical stability, and so on. Among them, spinel ternary oxide $MgGa_2O_4$ semiconductor, with large optical bandgap of 4.7–5.36 eV at room temperature, has good mechanical properties, high thermo-chemical stability at high temperature and high radiation hardness, making it suitable for SBUV photodetector application.[19–23]

However, $MgGa_2O_4$ was well known as a good luminescence material, and the luminescence properties of $MgGa_2O_4$ doped with Mn, Cr, Eu, and Ni have been intensively investigated to realize green, red, or near-infrared light emission under specific light irradiation.[23–26] Recently, the breakthrough in the fabrication of bulk $MgGa_2O_4$ single crystals has promoted its research and application as a transparent semiconductor oxide and an epitaxial substrate.[20] At the same time, owing to the excellent electrical and optical characteristics, $MgGa_2O_4$ has been regarded as an emerging semiconductor for high performance devices.[18,19] However, only very few $MgGa_2O_4$-based semiconductor devices, including gas sensors[27] and spintronic devices,[22,28] have been reported so far. No information is available about optoelectronic devices based on $MgGa_2O_4$, including a SBUV photodetector.

In this study, we report on the epitaxial growth of $MgGa_2O_4$ films by metal organic chemical vapor deposition (MOCVD) and the properties of their metal–semiconductor–metal (MSM) SBUV photodetectors. The structural, optical, and morphological properties of the films have been investigated before and after annealing in oxygen (O_2) or nitrogen (N_2) atmosphere. Additionally, the effect of high-temperature annealing of $MgGa_2O_4$ films on the performance of the SBUV detectors was also studied. Clearly, compared with devices based on as-grown and N_2-annealed thin films, the SBUV detector based on the O_2-annealed $MgGa_2O_4$ film has the lowest leakage current (~17 pA at a bias of 10 V) and the fastest response speed (t_r = 20 ns, t_d = 400 ns). The detailed mechanism for this phenomenon was subsequently discussed. Our findings in this work suggest that $MgGa_2O_4$ is an ideal candidate material for SBUV detection and has broad application prospects.

$MgGa_2O_4$ thin films were grown on *c*-plane sapphire substrates by MOCVD. Biscyclopentadienyl-Mg (Cp_2Mg), triethylgallium (TEGa), and high-purity oxygen gas were used as the magnesium, gallium, and oxygen precursors, respectively. High-purity nitrogen gas was selected as the carrier gas. The thin films were grown under a substrate temperature of 650 °C with a chamber pressure of 3000 Pa. The flow rates of Cp_2Mg, TEGa, and oxygen were kept at 10, 2, and 200 sccm, respectively. After the growth, $MgGa_2O_4$ films were annealed at a temperature of 900 °C in an O_2 or N_2 atmosphere for 1 h. The optical, structural, and surface morphology properties of $MgGa_2O_4$ films were characterized by adopting an UV-3101 PC scanning spectrophotometer, a Bruker D8GADDS x-ray diffractometer (XRD), and a scanning electron microscope (SEM) (HITACHI S-4800). Qualitative and quantitative analyses of the elements of the films were characterized by X-ray Photoelectron Spectroscopy (XPS) (Thermo ESCALAB 250). To further investigate the SBUV photodetection performance of the $MgGa_2O_4$ films with and without annealing, Au interdigital electrodes were fabricated on the films by photolithography and liftoff technology, thus realizing $MgGa_2O_4$ MSM photodetectors. The current–voltage (*I–V*) characteristic curves and time-dependent photocurrent (*I–t*) curves of the devices were measured by a semiconductor device analyzer (Agilent B1500A). The measurements of transient response characteristic and spectral response characteristic were carried out by using an oscilloscope, a Nd: YAG laser (245 nm), and a 200 W UV-enhanced Xe lamp with a monochromator.

Figure 1(a) shows the XRD patterns of as-grown, N_2-annealed, and O_2-annealed $MgGa_2O_4$ thin films on the *c*-face sapphire substrate. The strong and sharp peak that presents at $2\theta = 41.68°$ can be indexed as a (0006) peak of the *c*-Al_2O_3 substrate. In addition, all samples have three weak diffraction peaks at about $2\theta = 18.6°$, 37.8°, and 58°, which correspond exactly to the (111), (222), and (333) diffraction planes of the spinel $MgGa_2O_4$ (JCPDS No. 73–1721), respectively. It indicates that the $MgGa_2O_4$ films have a preferred growth orientation along the [111] direction. In addition, there is almost no change in the position of the diffraction peak after annealing. To further investigate the crystalline quality of $MgGa_2O_4$ films with and without annealing, high resolution XRD measurements have been performed as shown in Fig. 1(c). The full width at half maximum (FWHM) of the $MgGa_2O_4$ (222) peak of XRD rocking curve was estimated to be 0.15885°, 0.05068°, and 0.04191° for the as-grown, O_2-annealed, and N_2-annealed thin films, respectively. According to the previous reports, the high temperature annealing can help the lattice atoms to obtain enough energy to migrate to the appropriate position and can release the stress and reduce the dislocations and grain boundaries in the films.[29,30] Therefore, the decrease in the FWHM indicates that the crystalline quality could be significantly improved by the post-annealing at high temperature both in N_2 and O_2 atmospheres.

Figures 2(a), 2(b), and 2(c) present the top-view and the cross-sectional view SEM images of as-grown, O_2-annealed, and N_2-annealed $MgGa_2O_4$ thin films, respectively. It can be seen that all three films exhibit a granular surface morphology with a thickness of ~200 nm.

The optical transmission spectra of the $MgGa_2O_4$ films with and without annealing are shown in Fig. 2(d). The as-grown $MgGa_2O_4$ film exhibits an average transmittance of ~75% in the wavelength range from 300 to 700 nm. After high temperature annealing in N_2 and O_2 atmospheres, the average transmittance of the samples for the 300–700 nm wavelength range increases obviously to ~85%. In

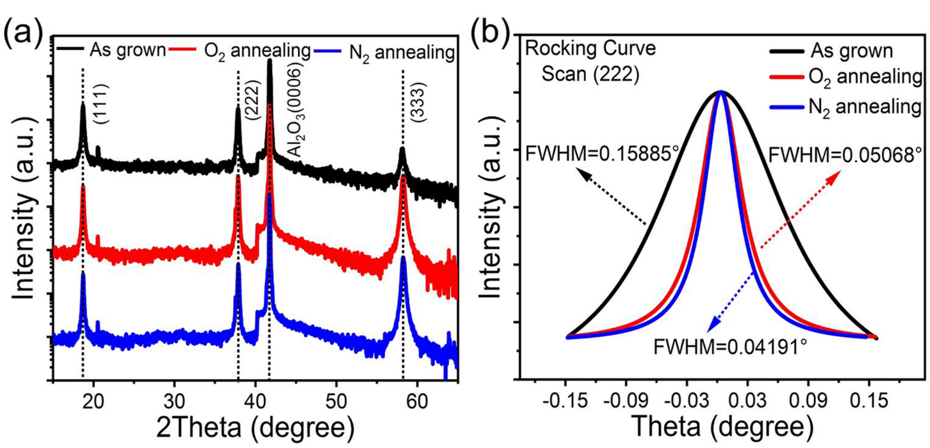

FIG. 1. (a) XRD patterns and (b) normalized XRD rocking curves of (222) plane of $MgGa_2O_4$ films with and without annealing.

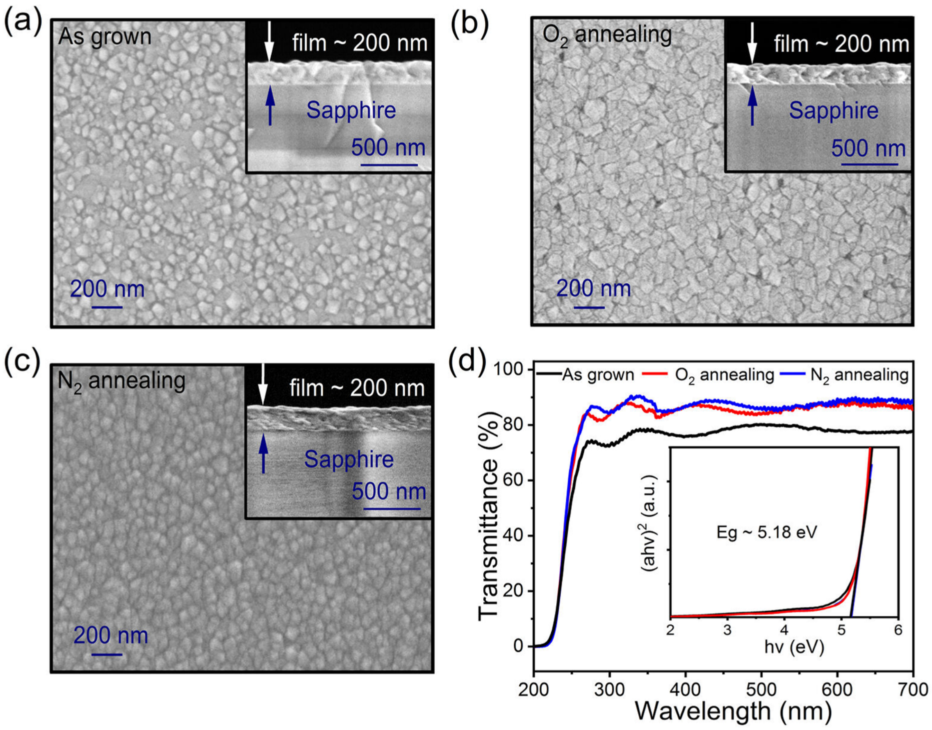

FIG. 2. Top view and cross-sectional view SEM images of (a) as-grown, (b) O_2-annealed, and (c) N_2-annealed $MgGa_2O_4$ films on the sapphire substrate. (d) Optical transmission spectra of the $MgGa_2O_4$ film with and without annealing. The inset shows a plot of $(\alpha h\nu)^2$ as a function of photon energy ($h\nu$).

addition, a sharp absorption edge can be observed at ~240 nm for all three samples, corresponding to an optical bandgap of ~5.18 eV as shown in the inset of Fig. 2(d).

According to the previous reports, the oxygen vacancy defects in the oxide semiconductors strongly affect their optical, electrical, and optoelectrical properties.[31,32] To investigate the chemical states and element composition of the $MgGa_2O_4$, XPS measurement was performed and the high resolution O1s XPS spectra were collected for $MgGa_2O_4$ films with and without annealing as shown in Fig. 3. The photoelectron energy scale was calibrated using C1s line at 284.6 eV. Obviously, the O1s peak can be consistently fitted by two near Gaussian components, centered at about 530.5 eV (O_I) and 531.8 eV (O_{II}), which are related to lattice oxygen (O^{2-}) and oxygen vacancies (V_o), respectively.[27,33] As can be observed, the relative ratios of the O_{II} peaks of as-grown, O_2-annealed, and N_2-annealed $MgGa_2O_4$ films are 30.64%, 15.21%, and 34.06%, respectively. This result clearly indicates that the concentration of oxygen vacancies in $MgGa_2O_4$ decreased after annealing in oxygen atmosphere. In contrast, high-temperature N_2 annealing could result in a slight increase in the V_o content.

In order to further study the UV detection performance of $MgGa_2O_4$ films, the MSM SBUV detectors with 25 pairs of Au interdigital electrodes (50 nm thickness) were fabricated using conventional photolithography and liftoff technology as shown in Fig. 4(a). The finger width and spacing of the interdigital electrodes are both 10 μm with a length of 1 mm. The *I–V* characteristics of the $MgGa_2O_4$ SBUV photodetectors measured in the dark are depicted in Fig. 4(b). The

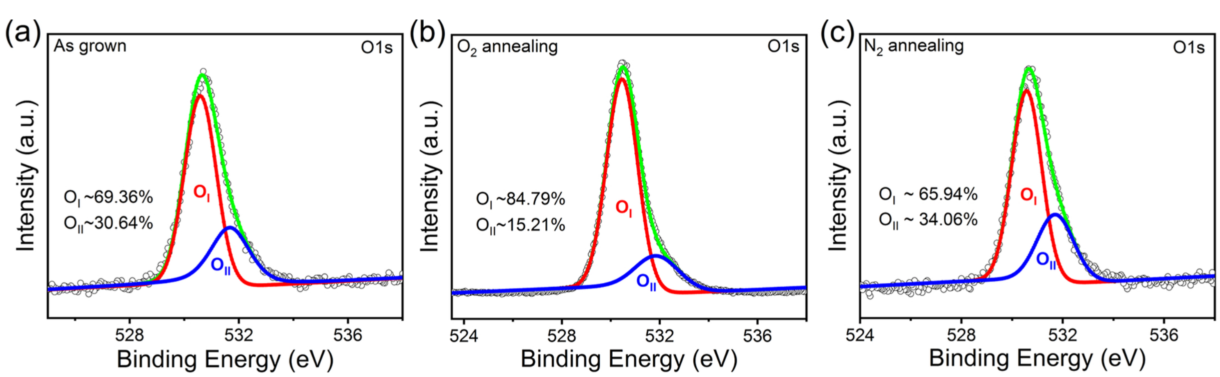

FIG. 3. XPS spectra of the O1s core level line for (a) as-grown, (b) O_2-annealed, and (c) N_2-annealed $MgGa_2O_4$ films.

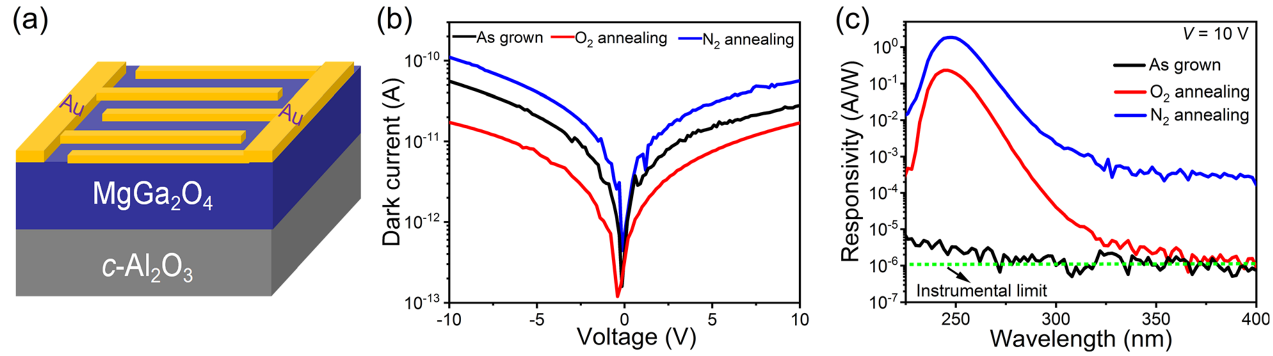

FIG. 4. (a) Schematic illustration of the SBUV MSM PDs based on $MgGa_2O_4$ films. (b) Dark I–V curves of $MgGa_2O_4$ SBUV PDs. (c) The spectral response of the SBUV PDs under 10 V bias with y axis in logarithmic scale.

Schottky contacts were formed between the $MgGa_2O_4$ film and the Au electrodes. Under 10 V bias, the dark currents of the devices based on as-grown, O_2-annealed, and N_2-annealed $MgGa_2O_4$ films are 54, 17, and 106 pA, respectively. Since oxygen vacancies are typical donor defects, the difference in the dark current should be related to the concentration of oxygen vacancies in $MgGa_2O_4$ films.[20] Figure 4(c) represents the spectral response of the $MgGa_2O_4$ SBUV PDs at a bias of 10 V. Notably, a very small responsivity of only several μA/W can be observed in the wavelength range of 225–270 nm for the as-grown $MgGa_2O_4$ photodetector. In contrast, the N_2-annealed and O_2-annealed devices show a large peak responsivity of about 1.84 and 0.23 A/W at $\sim$248 nm with a -3 dB cutoff wavelength of $\sim$255 nm, respectively. The higher responsivity of N_2-annealed $MgGa_2O_4$ may be associated with the trapping of photo-generated holes at neutral oxygen vacancies, which leads to a photoconductive gain. In addition, the O_2-annealed device possesses the higher UV-Vis rejection ratio ($R_{peak}/R_{400\,nm}$), which is more than 5 orders of magnitude. This phenomenon can be attributed to the large reduction of oxygen vacancy defects in $MgGa_2O_4$ after O_2 annealing, because oxygen vacancies often cause visible light absorption and response.

The I–t characteristics curves were measured by periodically turning on and off 254 nm (light intensity 500 μW/cm^2) light at a bias of 10 V. As shown in Fig. 5(a), the as-grown $MgGa_2O_4$ SBUV PD shows a weak response to the 254 nm light with poor stability and reproducibility. After annealing, the photocurrent of the devices significantly increased, and a good repeatability can be clearly observed [see Figs. 5(b) and 5(c)]. More interestingly, under (500 μW/cm^2) 254 nm light illumination at 10 V bias, the light-to-dark current ratio (I_{light}/I_{dark}) is as high as $\sim 1 \times 10^6$ for the O_2-annealed $MgGa_2O_4$ photodetector, while I_{light}/I_{dark} of the as-grown and N_2-annealed devices are $\sim$1.1 and $\sim 5 \times 10^5$, respectively.

To further investigate the response speed of the devices, the transient photoresponse measurement was carried out using a Nd:YAG pulsed laser with a wavelength of 245 nm. The laser pulse width and the frequency are 10 ns and 10 Hz, respectively. As shown in Figs. 6(a) and 6(c), both O_2-annealed and N_2-annealed $MgGa_2O_4$ SBUV photodetectors have a very fast, highly stable, and reproducible response to the SBUV light. The 10%–90% rise time and 90%-10% decay time of O_2-annealed device are around 20 and 400 ns, respectively, as shown in Fig. 6(b). As for N_2-annealed device, its 10%–90% rise time and 90%-10% decay time are around 80 ns and 30 μs, respectively. Notably, in Fig. 6(d), the decay portion of the transient response exhibits two distinct phases: a fast initial decay followed by a much slow decay. The slow decay should be associated with large amounts of oxygen vacancy defects in $MgGa_2O_4$ after annealing in N_2 atmosphere.

In summary, we have demonstrated the spinel ternary oxide $MgGa_2O_4$ thin films on the c-plane sapphire substrate using MOCVD. After post annealing in O_2 or N_2 atmosphere, the crystalline quality of $MgGa_2O_4$ thin films was improved obviously. The O_2-annealed $MgGa_2O_4$ film has a lower oxygen vacancy defect concentration

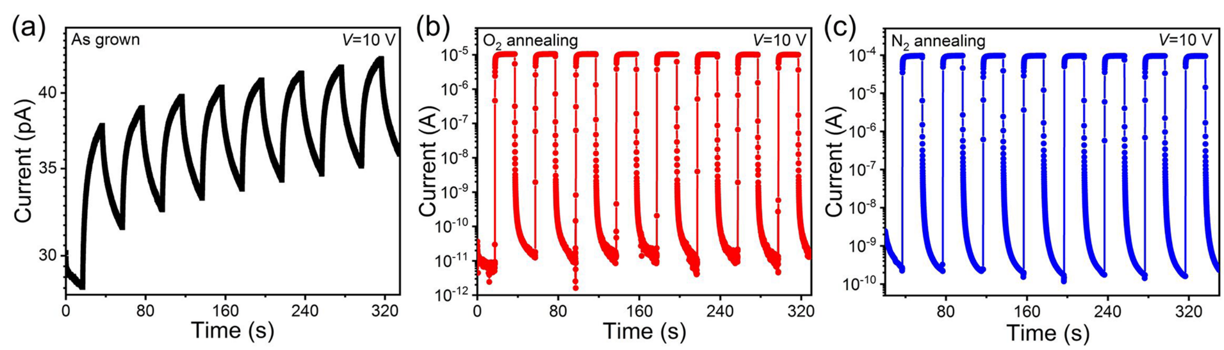

FIG. 5. I–t characteristics of (a) as-grown, (b) O_2-annealed, and (c) N_2-annealed $MgGa_2O_4$ SBUV photodetectors under 254 nm light illumination with an intensity of 500 μW/cm^2 at 10 V.

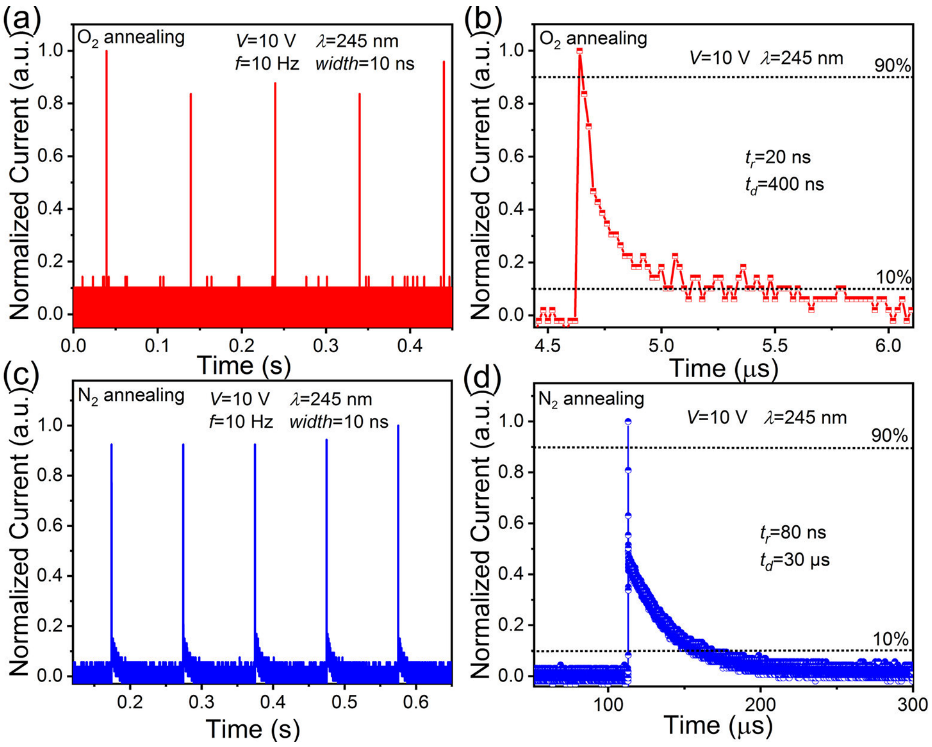

FIG. 6. Normalized transient photoresponse curves of the O_2-annealed [(a) and (b)] and N_2-annealed [(c) and (d)] $MgGa_2O_4$ SBUV photodetectors.

compared to the as-grown and N_2-annealed samples. In addition, an excellent SBUV photodetection performance has been observed for O_2-annealed $MgGa_2O_4$ film. The dark current of the MSM SBUV photodetector based on O_2-annealed $MgGa_2O_4$ was only about 17 pA at a bias of 10 V, and the peak responsivity was 0.23 A/W at ~248 nm with a −3 dB cutoff wavelength of ~255 nm. In addition, the UV-Vis rejection ratio ($R_{peak}/R_{400\,nm}$) is more than 5 orders of magnitude, which may be related to the suppression of visible light response by the reduction of defects after oxygen annealing. Our findings in this work indicate that $MgGa_2O_4$ spinel is a promising candidate for realizing high-performance SBUV photodetection.

This work was supported by the National Natural Science Foundation of China (Nos. 62074148, 61875194, 11727902, 12074372, 11774341, 11974344, 61975204, and 11804335), the 100 Talents Program of the Chinese Academy of Sciences, Youth Innovation Promotion Association, CAS (No. 2020225).

AUTHOR DECLARATIONS

Conflict of Interest

The authors have no conflicts of interest to disclose.

DATA AVAILABILITY

The data that support the findings of this study are available from the corresponding author upon reasonable request.

REFERENCES

[1]R. Suzuki, S. Nakagomi, and Y. Kokubun, Appl. Phys. Lett. **98**, 131114 (2011).
[2]J. J. Xu, W. Zheng, and F. Huang, J. Mater. Chem. C **7**, 8753 (2019).
[3]X. Zhou, Q. Zhang, L. Gan, X. Li, H. Q. Li, Y. Zhang, D. Golberg, and T. Y. Zhai, Adv. Funct. Mater. **26**, 704 (2016).
[4]S. Rathkanthiwar, A. Kalra, S. V. Solanke, N. Mohta, R. Muralidharan, S. Raghavan, and D. N. Nath, J. Appl. Phys. **121**, 164502 (2017).
[5]Y. R. Chen, Z. W. Zhang, H. Jiang, Z. M. Li, G. Q. Miao, and H. Song, J. Mater. Chem. C **6**, 4936 (2018).
[6]Q. Cai, H. F. You, H. Guo, J. Wang, B. Liu, Z. L. Xie, D. J. Chen, H. Lu, Y. D. Zheng, and R. Zhang, Light-Sci. Appl. **10**, 94 (2021).
[7]H. Y. Chen, P. P. Yu, Z. Z. Zhang, F. Teng, L. X. Zheng, K. Hu, and X. S. Fang, Small **12**, 5809 (2016).
[8]S. Han, Z. Z. Zhang, J. Y. Zhang, L. K. Wang, J. Zheng, H. F. Zhao, Y. C. Zhang, M. M. Jiang, S. P. Wang, D. X. Zhao, C. X. Shan, B. H. Li, and D. Z. Shen, Appl. Phys. Lett. **99**, 242105 (2011).
[9]B. Zhao, F. Wang, H. Y. Chen, L. X. Zheng, L. X. Su, D. X. Zhao, and X. S. Fang, Adv. Funct. Mater. **27**, 1700264 (2017).
[10]X. H. Chen, F. F. Ren, S. L. Gu, and J. D. Ye, Photonics Res. **7**, 381 (2019).
[11]X. Chen, K. W. Liu, Z. Z. Zhang, C. R. Wang, B. H. Li, H. F. Zhao, D. X. Zhao, and D. Z. Shen, ACS Appl. Mater. Interfaces **8**, 4185 (2016).
[12]N. Susilo, S. Hagedorn, D. Jaeger, H. Miyake, U. Zeimer, C. Reich, B. Neuschulz, L. Sulmoni, M. Guttmann, F. Mehnke, C. Kuhn, T. Wernicke, M. Weyers, and M. Kneissl, Appl. Phys. Lett. **112**, 041110 (2018).
[13]M. M. Fan, K. W. Liu, Z. Z. Zhang, B. H. Li, X. Chen, D. X. Zhao, C. X. Shan, and D. Z. Shen, Appl. Phys. Lett. **105**, 011117 (2014).
[14]X. H. Xie, Z. Z. Zhang, C. X. Shan, H. Y. Chen, and D. Z. Shen, Appl. Phys. Lett. **101**, 081104 (2012).
[15]C. L. Lu, Q. Y. Zhang, S. Li, Z. Y. Yan, Z. Liu, P. G. Li, and W. H. Tang, J. Phys. D **54**, 405107 (2021).
[16]D. Y. Han, K. W. Liu, Q. C. Hou, X. Chen, J. L. Yang, B. H. Li, Z. Z. Zhang, L. Liu, and D. Z. Shen, Sens. Actuator, A **315**, 112354 (2020).
[17]C. Y. Yan, N. Singh, and P. S. Lee, Appl. Phys. Lett. **96**, 053108 (2010).
[18]L. Li, P. S. Lee, C. Y. Yan, T. Y. Zhai, X. S. Fang, M. Y. Liao, Y. Koide, Y. Bando, and D. Golberg, Adv. Mater. **22**, 5145 (2010).
[19]C. Hirschle, J. Schreuer, and Z. Galazka, J. Appl. Phys. **124**, 065111 (2018).

[20]Z. Galazka, D. Klimm, K. Irmscher, R. Uecker, M. Pietsch, R. Bertram, M. Naumann, M. Albrecht, A. Kwasniewski, R. Schewski, and M. Bickermann, Phys. Status Solidi A **212**, 1455 (2015).
[21]B. Thielert, C. Janowitz, Z. Galazka, and M. Mulazzi, Phys. Rev. B **97**, 235309 (2018).
[22]H. Sukegawa, Y. Kato, M. Belmoubarik, P. H. Cheng, T. Daibou, N. Shimomura, Y. Kamiguchi, J. Ito, H. Yoda, T. Ohkubo, S. Mitani, and K. Hono, Appl. Phys. Lett. **110**, 122404 (2017).
[23]A. Mondal, S. Das, and J. Manam, RSC Adv. **6**, 82484 (2016).
[24]G. K. B. Costa, S. S. Pedro, I. C. S. Carvalho, and L. P. Sosman, Opt. Mater. **31**, 1620 (2009).
[25]A. Luchechko, Y. Shpotyuk, O. Kravets, O. Zaremba, K. Szmuc, J. Cebulski, A. Ingram, R. Golovchak, and O. Shpotyuk, J. Adv. Ceram. **9**, 432 (2020).
[26]T. Suzuki, G. S. Murugan, and Y. Ohishi, J. Lumin. **113**, 265 (2005).
[27]L. F. He, C. P. Gao, L. Yang, K. Zhang, X. F. Chu, S. M. Liang, and D. W. Zeng, Sens. Actuators, B **306**, 127453 (2020).
[28]K. Nawa, K. Masuda, and Y. Miura, Phys. Rev. B **102**, 144423 (2020).
[29]S. Hagedorn, S. Walde, N. Susilo, C. Netzel, N. Tillner, R. Unger, P. Manley, E. Ziffer, T. Wernicke, C. Becker, H. Lugauer, M. Kneissl, and M. Weyers, Phys. Status Solidi A **217**, 1900796 (2020).
[30]H. Miyake, G. Nishio, S. Suzuki, K. Hiramatsu, H. Fukuyama, J. Kaur, and N. Kuwano, Appl. Phys. Exp. **9**, 025501 (2016).
[31]F. Gunkel, D. V. Christensen, Y. Z. Chen, and N. Pryds, Appl. Phys. Lett. **116**, 120505 (2020).
[32]M. V. Ganduglia-Pirovano, A. Hofmann, and J. Sauer, Surf. Sci. Rep. **62**, 219 (2007).
[33]X. Zhou, B. Q. Wang, H. B. Sun, C. Wang, P. Sun, X. W. Li, X. L. Hu, and G. Y. Lu, Nanoscale **8**, 5446 (2016).